

On evaluation of influence coefficients for edge and intermediate boundary elements in 3D problems involving strong field concentrations

L. RYBARKA-RUSINEK *

Rzeszow University of Technology, Poland

Abstract. The paper presents a tool for accurate evaluation of high field concentrations near singular lines, such as contours of cracks, notches and grains intersections, in 3D problems solved the BEM. Two types of boundary elements, accounting for singularities, are considered: (i) edge elements, which adjoin a singular line, and (ii) intermediate elements, which while not adjoining the line, are still under strong influence of the singularity. An efficient method to evaluate the influence coefficients and the field intensity factors is suggested for the both types of the elements. The method avoids time expensive numerical evaluation of singular and hypersingular integrals over the element surface by reduction to 1D integrals. The method being general, its details are explained by considering a representative examples for elasticity problems for a piecewise homogeneous medium with cracks, inclusions and pores. Numerical examples for plane elements illustrate the exposition. The method can be extended for curvilinear elements.

Key words: boundary integral equation, boundary element method, singular element, Hadamard finite part integral.

1. Introduction

For wide range of scientific, engineering and technological problems it is of significance to increase the quality of modeling in regions of strong field concentration, such as a vicinity of common edges of neighbouring elements, corners, notches, fracture fronts, intersections of structural elements, places with changes of boundary or contact conditions [1–5]. The presence of “singular points” and “singular lines” causes unfavourable physical processes and leads to computational difficulties when numerically simulating their influence. For these reasons, in the theoretical physics, mechanics and engineering sciences, great attention is paid to the studies of the singularities. In parallel with the mathematical theory, focusing on formal investigations in abstract spaces, such as the Sobolev space [6], there are researches aimed to efficiently evaluate exponents in asymptotic equations describing behaviour of fields near singularities and to employ them for solving engineering problems [8–11]. Most of the publications contain numerical results merely for the simplest particular cases, such as a crack tip, notch, and common apex of two wedges. The way for efficient, accurate and stable finding the asymptotics for an arbitrary configuration of wedges was suggested in [12]; it was further developed and employed in a robust subroutine in [13]. Extensions to thin contact layers and to functionally graded wedges are given in the papers [14–17]. Therefore, to the date, the problem of numerical evaluation of the asymptotic exponent is actually solved as concerns with two-dimensional problems. For them, the developed methods of evaluation and

accounting for asymptotics near singular points have been already employed for strongly inhomogeneous media with multiple singular points [18]. For three-dimensional problems, because of great mathematical and computational difficulties, especially as regards to hypersingular integrals, available solutions have referred to the simplest singularity, corresponding to cracks in a homogeneous medium, when the exponent of the asymptotics is $1/2$ (e.g. [19–21]). Results of numerical experiments presented in [21] show that using special edge elements (with square root density approximation) in frames of Boundary Element Method (BEM), based on hypersingular boundary integral equations (BIE), specially derived for 3D piecewise homogeneous media, significantly increases the accuracy of evaluation of stress intensity factors (SIFs). However, there are many three-dimensional engineering problems, which require accounting for more general types of asymptotics, when the exponent α of the power asymptotic may be an arbitrary number in the interval $(0, 1)$. Such asymptotics are common in fracture mechanics at a vicinity of points at neighbouring edges of structural elements with different elastic properties; at contours of cracks propagating at the boundaries of inhomogeneities, in hydraulic fracturing (specifically, $\alpha = 2/3$ for the viscosity dominated regime of fracture propagation [22]; $\alpha = 5/8$ for the leak-off dominated regime [23]). Thus, there is a need to extend an approach suggested in [21] for $\alpha = 1/2$ to an arbitrary α . The paper aims to make extension for elements near the singular line: edge elements and intermediate elements. In literature on 3D hydraulic fractures (e.g. [24]) those elements are called, respectively, tip and ribbon elements. The method of efficient evaluation of influence coefficients is given below for such elements with density of the form cr^α , where r is the distance from a singular line, c is a constant and α is an arbitrary number in the interval $(0, 1)$. It tends to make a step in notable increasing quality of numerical simulation of local fields.

*e-mail: rybarska@prz.edu.pl

Manuscript submitted 2018-02-06, revised 2018-07-17, initially accepted for publication 2018-08-09, published in February 2019.

2. Problem formulation

For certainty, consider a domain of P isotropic elastic blocks, characterized by the shear modulus μ_p , and the same Poisson's ratios $\nu_p = \nu$ ($p = 1, 2, \dots, P$) and containing cracks, pores and inclusions of arbitrary shapes. Denote S the total boundary of all the blocks and surfaces of cracks, pores and inclusions. The boundary between adjacent blocks is treated as a single surface on which physical fields may experience discontinuities. Problems for such strongly inhomogeneous medium can be solved by applying the BEM (e.g. [25]) to specially tailored singular and hypersingular BIE [26]. Special attention should be paid to contours L of cracks and to intersections of grain surfaces because the fields are singular in their vicinity. Thus when discretizing the total surface S , it is reasonable to distinguish boundary elements, which are under the influence of the asymptotics generated by the singular lines. For instance, such a line L may be the contour of the cap crack surface S shown in Fig. 1. In addition to conventional boundary elements (e.g. [25]), shown in white, we consider two specific groups of elements. They serve to account for fast change of physical quantities in the zone of strong influence of asymptotics ("asymptotic umbrella"). The first group consists of elements adjoining the contour L . These are *edge* elements; they are shown in dark in Fig. 1. The other group are elements, which are still under the asymptotic umbrella, while not having points on the singular line. These are *intermediate* elements; they are shown in grey in Fig. 1. As mentioned, in papers on hydraulic fractures, these two groups of elements, are called respectively, tip and ribbon elements.

After representing the boundary S by M boundary elements S^q of the three types, the BIE is [21, 26]:

$$\sum_{q=1}^M \int_{S^q} \mu U(x^j, \xi) \Delta t_n(\xi) ds_\xi - \sum_{q=1}^M \int_{S^q} U_S(x^j, \xi) (\mu^+ u^+(\xi) - \mu^- u^-(\xi)) ds_\xi = \frac{1}{2} (\mu^+ u^+(x^j) + \mu^- u^-(x^j)), \quad x^j \in S \quad j = 1, 2, \dots, N, \quad (1)$$

$$\sum_{q=1}^M \int_{S^q} \left(\frac{1}{2\mu^+} J_S^+(x^j, \xi) t_n^+(\xi) - \frac{1}{2\mu^-} J_S^-(x^j, \xi) t_n^-(\xi) \right) ds_\xi + \sum_{q=1}^M \int_{S^q} \frac{1}{2\mu} J_H(x^j, \xi) \Delta u(\xi) ds_\xi = \frac{1}{2} \left(\frac{1}{2\mu^+} t_n^+(x^j) + \frac{1}{2\mu^-} t_n^-(x^j) \right), \quad x^j \in S \quad j = 1, 2, \dots, N, \quad (2)$$

where $\Delta t_n = t_n^+ - t_n^-$ is the traction discontinuity; $\Delta u = u^+ - u^-$ is the displacement discontinuity, $x^j \in S$ is a field (collocation) point (the number N of these points is taken equal to the number of unknowns in approximations of the densities in the integrals entering (1), (2)). The normal $n(y)$ is fixed arbitrary on a contact of adjacent blocks, on cracks and inclusions. The index "plus" ("minus") refers to the limiting value from the side with respect to which the normal n is outward (inward).

The elements of the matrix $U(x, \xi)$ of fundamental solutions, defined by the Kelvin's solution are:

$$(U(x, \xi))_{ij} = \frac{1}{16\pi\mu_p(1-\nu)} \left[(3-4\nu) \frac{\delta_{ij}}{R} + \frac{R_i R_j}{R^3} \right], \quad (3)$$

where $\sqrt{(x_i - \xi_i)^2}$, $i = 1, 2, 3$ is the distance between a field point x and integration point ξ . Summation over repeated Latin index is assumed henceforth. The matrix J_S is obtained by applying the traction operator $T_{n(x)}$ to the matrix U :

$$(J_S(x, \xi))_{ij} = (T_{n(x)} U(x, \xi))_{ij} = \frac{1}{8\pi(1-\nu)} \left[(1-2\nu) \frac{n_i(x) R_j - R_k n_k(x) \delta_{ij} - R_i n_j(x) - 3 \frac{R_i R_k n_k(x) R_j}{R^5}}{R^3} \right]. \quad (4)$$

The matrix

$$U_S(x, \xi) = [J_S(x, \xi)]^T \quad (5)$$

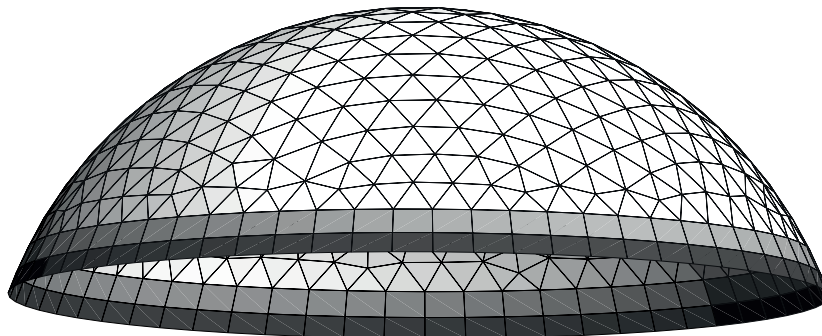


Fig. 1. Approximation of the surface by ordinary (white), edge (dark) and intermediate (grey) elements

defines the kernel of the potential of double-layer.

The hypersingular matrix J_H is defined as $J_H(x, \xi) = T_{n(x)}(J_S(x, \xi))^T$. For the Kelvin solution its components are:

$$\begin{aligned}
 (J_H(x, \xi))_{ij} = & \\
 & \frac{\mu_p}{4\pi(1-\nu)} \left\{ \frac{(1-2\nu)[n_k(x)n_k(\xi)\delta_{ij} + n_i(\xi)n_j(x)]}{R^3} \right. \\
 & - \frac{(1-4\nu)n_i(x)n_j(\xi)}{R^3} + \\
 & + \frac{3(1-2\nu)[R_k n_k(\xi)n_i(x)R_j + R_k n_k(x)R_i n_j(\xi)]}{R^5} + \\
 & + \frac{3\nu R_l n_l(\xi)[R_k n_k(x)\delta_{ij} + R_i n_j(x)]}{R^5} + \\
 & + \frac{3\nu R_j [n_k(x)n_k(\xi)R_i + R_k n_k(x)n_i(\xi)]}{R^5} + \\
 & \left. - \frac{15R_k n_k(x)R_l n_l(\xi)R_i R_j}{R^7} \right\}. \quad (6)
 \end{aligned}$$

The integrals with these kernels over ordinary elements are evaluated for densities approximated by smooth functions, commonly polynomials (e.g. [20, 27]). In this paper, we focus on evaluation of integrals over edge and intermediate elements. For them, the densities are approximated by functions accounting for the asymptotic behaviour of fields in the vicinity of a singular line L .

Note that the results for these kernels are also of use when employing the extended finite element method (XFEM, see, e.g. [24, 28]).

3. Method of integration

3.1. Approximation of density function. In further discussion we assume that the edge and intermediate elements are plane having in mind that a curvilinear element may be transformed to a planar element by smooth transformation of spatial variables (the Jacobian is included into a density). A planar element is taken as trapezoid, which in particular cases becomes a rectangle, a square, or a triangle. For a plane element, it is convenient to perform integration in the local Cartesian coordinates. Specifically, for an element T , the origin O and the axes y_2 and y_3 are located in its plane with the axis y_2 along the singular line (Fig. 2). The axis y_1 is taken in the direction of the normal n to the element.

The asymptotic behavior of the density, in quite general cases (see, e.g. [8, 11–17, 22, 23]), is of the form $O(y_3^\alpha)$ with $0 \leq \alpha < 1$. Thus the density is approximated as

$$f(y) = y_3^\alpha \left(c_0 + \sum_{k+l=1}^{m_p} c_{kl} y_2^k y_3^l \right) \quad (7)$$

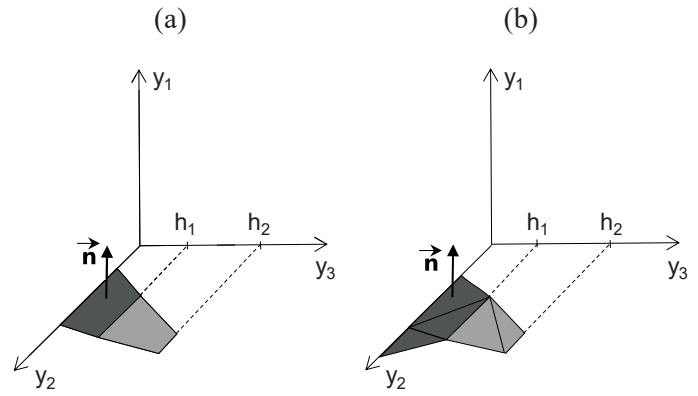


Fig. 2. Special a) trapezoidal and b) triangular elements in the local system of coordinates

with c_0 being the field intensity factor. The exponent α is pre-defined and evaluated in advance. In contrast, c_0 is found by solving the BIE. Specifically, in fracture mechanics, for a crack contour, $\alpha = 1/2$ and c_0 is proportional to the conventional stress intensity factor (see, e.g. [29]). In problems of hydraulic fracturing, c_0 is the opening intensity factor, which characterizes the speed of the fracture propagation (e.g. [30]) and it is found by solving the problem on time steps.

The case $\alpha = 0$ corresponds to a non-singular asymptotics. For it, an element is actually ordinary, and integration over it is performed by well-developed methods (e.g. [20, 21, 27]). Below we focus on edge and intermediate elements when $0 < \alpha < 1$. Then the only difference between edge and intermediate elements is that for the first of them $h_1 = 0$, while for the second $h_1 > 0$. Therefore, the both groups may be considered in the same way.

3.2. Reduction to one-dimensional integrals. A typical trapezoidal edge ($h_1 = 0$) or intermediate ($h_1 > 0$) element (Fig. 2) involves integration over the domain

$$T = \{(y_2, y_3) : h_1 < y_3 < h_2, \\ a_b y_3 + b_b < y_2 < a_f y_3 + b_f\}. \quad (8)$$

If a field point x belongs to T , the integrals are singular (Cauchy principal value or Hadamard finite part integrals). Otherwise the integrals are ordinary (Riemann integrals). For a fixed field point, the sum of integrals over an element presents the *influence coefficient* of this element on a physical quantity in the right hand side of (1) or (2) at the point x . We are looking for parts of the influence coefficients generated by particular integrals. The method to evaluate the integrals employs the specific geometry of the trapezoidal element: two of its sides are parallel to the y_2 axis. This serves to reduce the double integrals to iterated integrals, internal of which is integrated analytically. As a result, we arrive at one dimensional integrals, which in their turn, may be Riemann, Cauchy principal value or Hadamard finite part integrals. The latter are efficiently evaluated as explained below.

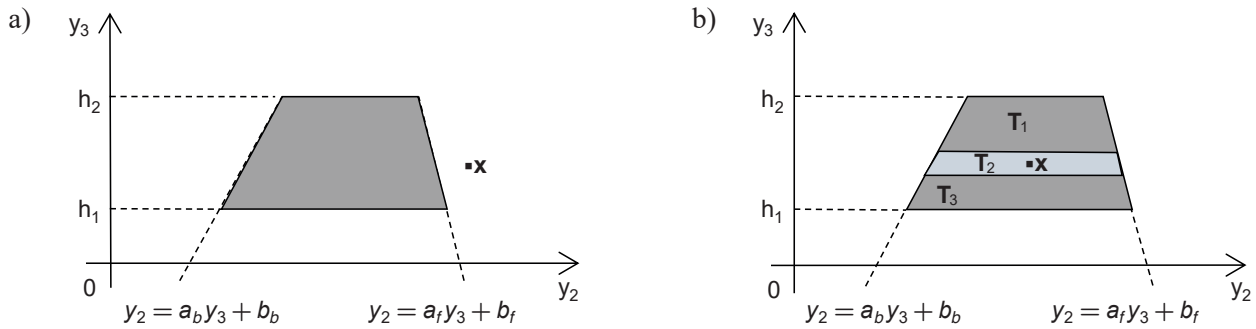


Fig. 3. Trapezoidal special element in the local system of coordinates with field point x located a) outside and b) inside element

Further on, to present the essence of the method and to show all its details we consider the representative hypersingular integral of the form

$$J_M = \iint_T \frac{y_3^\alpha dy_2 dy_3}{R^3}, \quad 0 < \alpha < 1. \quad (9)$$

Other integrals are either reduced to this integral, or evaluated in the same way. Note also that the integral (9) is the only integral to be evaluated when solving hydraulic fracture problems for a propagating planar crack (see, e.g. [24])

3.3. Evaluation of influence coefficients for representative integral. The integral (9) over an element T defined by (8) can be expressed as an iterative integral

$$J_M = \int_{h_1}^{h_2} y_3^\alpha \left(\int_{a_b y_3 + b_b}^{a_f y_3 + b_f} \frac{dy_2}{\left(\sqrt{x_1^2 + (x_2 - y_2)^2 + (x_3 - y_3)^2} \right)^3} \right) dy_3, \quad (10)$$

where $x = (x_1, x_2, x_3)$ is a field point.

The inner integral in (10) is promptly evaluated by writing dy_2 as $-d(x_2 - y_2)$ and accounting that the antiderivative of $F(x) = \frac{1}{(\sqrt{x^2 + A^2})^3}$ is $\frac{x}{A^2 \sqrt{x^2 + A^2}}$. Then (10) is reduced to the one dimensional integral:

$$\int_{h_1}^{h_2} \frac{-y_3^\alpha}{x_1^2 + (x_3 - y_3)^2} \left[\frac{(x_2 - y_2)}{\sqrt{x_1^2 + (x_2 - y_2)^2 + (x_3 - y_3)^2}} + C \right]_{a_b y_3 + b_b}^{a_f y_3 + b_f} dy_3, \quad (11)$$

where $[G(x)]_a^b$ denotes double substitution $G(b) - G(a)$, C is a constant to be chosen as convenient.

There are three special cases to be considered.

First case. The inequality $x_1^2 + (x_3 - y_3)^2 > 0$ is fulfilled for all $h_1 \leq y_3 \leq h_2$. In this simplest situation the integrand is a continuous function and the integral (11) may be found by using conventional numerical technique e.g. the Gaussian quadrature rule.

Second case. The field point $x = (0, x_2, x_3)$ is located in the trapezoid plane ($x_1 = 0$) in the strip between the lines $y_3 = h_1$ and $y_3 = h_2$, while outside the trapezoid (Fig. 3a). In this case, by setting $C = -\text{sign}(x_2 - a_b x_3 - b_b)$, we have $C = 1$ ($C = -1$) when the point x is to the left (right) of the trapezoid. By using this value of C in equation (11) we avoid artificial singularity, which appears if taking $C = 0$. Then, as it should be, the integral J_M is the Riemann's integral:

$$\int_{h_1}^{h_2} \left[\frac{y_3^\alpha}{\sqrt{(x_2 - y_2)^2 + (x_3 - y_3)^2} \left((x_2 - y_2) - C \sqrt{(x_2 - y_2)^2 + (x_3 - y_3)^2} \right)} \right]_{y_2 = a_b y_3 + b_b}^{y_2 = a_f y_3 + b_f} dy_3.$$

It is evaluated similar to that in the *First case*.

Third case. The field point x is located within the trapezoid. In this case, the integral (9) is the finite part Hadamard integral. If a density were a polynomial, the integral would be evaluated analytically. This suggests evaluation of (9) through expansion of y_3^α in Taylor series in $y_3 - x_3$ within a narrow strip $x_3 - \varepsilon x_3 < y_3 < x_3 + \varepsilon x_3$ with x_3 at its middle (Fig. 3b). The value of y_3^ε should be small enough to have the intersection of the strip with the trapezoid entirely within the latter: $0 < \varepsilon < \min_{i=1,2} \left| 1 - \frac{h_i}{x_3} \right|$.

A proper choice of a particular ε , satisfying this condition and providing accurate evaluation of the integral J_M , is left to the next Section. The Taylor expansion of y_3^ε is written as

$$y_3^\alpha = x_3^\alpha \left[1 - \alpha \left(1 - \frac{y_3}{x_3} \right) + \sum_{k=2}^n (-1)^k \frac{\alpha(\alpha-1)\dots(\alpha-k+1)}{k!} \left(1 - \frac{y_3}{x_3} \right)^k + O(\varepsilon^{n+1}) \right]. \quad (12)$$

With this prerequisite, the integral over trapezoid T is represented as the sum $J_M = J_1 + J_2 + J_3$ of integrals over the

narrow strip T_2 and the parts T_1 and T_3 , respectively, above and below the strip (Fig. 3b). The integrals over T_1 and T_3 are those considered in *First case*. The integral over T_2 is evaluated through substitution of the expansion (12):

$$J_2 = -\frac{1}{x_3^{1-\alpha}} \int_{1-\varepsilon}^{1+\varepsilon} \frac{1}{(1-\eta)^2} \cdot \left[\frac{\frac{x_2}{x_3} - \xi}{\sqrt{(\frac{x_2}{x_3} - \xi)^2 + (1-\eta)^2}} \right]_{\xi=a_b\eta+\frac{b_b}{x_3}}^{\xi=a_f\eta+\frac{b_b}{x_3}} d\eta + \frac{\alpha}{x_3^{1-\alpha}} \cdot \int_{1-\varepsilon}^{1+\varepsilon} \frac{1}{1-\eta} \left[\frac{\frac{x_2}{x_3} - \xi}{\sqrt{(\frac{x_2}{x_3} - \xi)^2 + (1-\eta)^2}} \right]_{\xi=a_b\eta+\frac{b_b}{x_3}}^{\xi=a_f\eta+\frac{b_b}{x_3}} d\eta + \sum_{k=2}^n (-1)^{k+1} \frac{\alpha(\alpha-1)\dots(\alpha-k+1)}{x_3^{1-\alpha} k!} + \int_{1-\varepsilon}^{1+\varepsilon} \left[\frac{(1-\eta)^{k-2} (\frac{x_2}{x_3} - \xi)}{\sqrt{(\frac{x_2}{x_3} - \xi)^2 + (1-\eta)^2}} \right]_{y_2=a_b y_3 + b_b}^{y_2=a_f y_3 + b_f} d\eta + O(\varepsilon^{n+1}),$$

where symbols \int , \int denote the finite part Hadamard and the Cauchy integrals, respectively. All the integrals in (13) are evaluated analytically with exact formulae for $n = 4$ given in *Appendix*. Clearly the quadrature rule (13) should be used with ε small enough. On the other hand, ε should not be too small, because when $\varepsilon \rightarrow 0$, the integrals J_1, J_3 tend to plus infinity, while the integral J_2 goes to minus infinity; then the method suggested fails. Therefore, it is crucial to properly select the parameters of the method to guarantee a prescribed accuracy with minimal computational cost.

4. Numerical experiments

There is no principal difference between integration over an intermediate and edge element. The latter presents a particular case of the former, corresponding to $h_1 = 0$. Therefore, below we consider the general case of an element ($h_1 \geq 0$). A number of numerical experiments (for edge and intermediate elements) were performed to study sensitivity of the method for the choice of parameter ε and order n of approximation. The typical results are presented below.

Choice of parameter ε . Consider in the local system a plane trapezoid T with vertices: $W_1 = (0, 1, 1)$, $W_2 = (0, 8, 1)$, $W_3 = (0, 6, 3)$, $W_4 = (0, 3, 3)$. The integral J_M is defined by (9) over T . When choosing the relative width 2ε of the narrow

strip, it is sufficient to set $\alpha = 0$ to exclude the error caused by approximation of y_3^α .

The field point $x = (0, 4, 2)$ is located inside the trapezoid and the integral is the Hadamard finite part integral. In the considered case of smooth density function, the error of evaluation of integral J_M by the method suggested is generated only by the division leading to the described evaluation of J_1 and J_3 via the Gaussian quadrature rule and J_2 via (13), in which the first term on the right hand side gives the exact value then $\alpha = 0$. The exact value of J_M , obtained analytically, is -4.40797014 ; it serves as a benchmark for a proper choice of the ε . The table presents approximate values of J_1, J_2, J_3 and J_M for $\varepsilon = 0.3$ (0.1, 0.05, 0.01) and with various number (5, 10, 16) of nodes in Gaussian quadratures. All calculations are performed with double precision. From Table 1 it appears that when the strip is very thin ($\varepsilon = 0.01$), the Riemann integrals J_1 and J_3 are strongly underestimated, what occurs even for 16-point Gaussian quadrature. This follows from the notable disagreement between the exact value of J_M and the value, given in the table, evaluated numerically for actually exact value of J_2 . Results show, that to have the accuracy at a satisfactory level, the relative height $\varepsilon = h/H$ of the thin strip should be in the range (0.05, 0.3) when using 10 or more points of Gaussian

Table 1
Values of integrals: J_1, J_2, J_3, J_M for $\alpha = 0$ and for different parameters of the method

	5-point quadrature	10-point quadrature	16-point quadrature
$\varepsilon = 0.3$			
J_1	1.2956913073	1.2956906655	1.2956906800
J_2	-6.8948619920	-6.8948619920	-6.8948619920
J_3	1.1912017293	1.1912011421	1.1912011555
J_M	-4.4079689554	-4.4079701844	-4.4079701565
$\varepsilon = 0.1$			
J_1	7.9036077572	7.9109116859	7.9109127578
J_2	-20.0726689106	-20.0726689106	-20.0726689106
J_3	7.7464807727	7.7537847824	7.7537858526
J_M	-4.4225803806	-4.4079724422	-4.4079703001
$\varepsilon = 0.05$			
J_1	17.5988320976	17.8942478294	17.8950976921
J_2	-40.0361665857	-40.0361665857	-40.0361665857
J_3	17.4368311918	17.7322470107	17.7330968716
J_M	-5.0005032964	-4.4096717457	-4.4079720220
$\varepsilon = 0.01$			
J_1	64.1534584621	93.6506221500	97.6527190735
J_2	-200.0072271415	-200.0072271415	-200.0072271415
J_3	63.9899011131	93.4870649002	97.4891618219
J_M	-71.8638675663	-12.8695400913	-4.8653462461

quadrature. For 16 points, such a choice of parameter ε guarantees the accuracy of five significant digits, at least.

Choice of order n of approximation. Consider in the local system a plane trapezoid T with the vertices: $W_1 = (0, 1, 2)$, $W_2 = (0, 4, 2)$, $W_3 = (0, 4, 3)$, $W_4 = (0, 2, 3)$ and integral J_M defined by (9) over T . The collocation point $x = (0, 3, 2.5)$ is located inside the domain. According to suggestions of the previous *Example*, the height of inner trapezoid T_2 is taken $h = 2 \cdot 0.05 H$. For lower J_1 and for upper J_3 integrals the 16-node Gaussian quadrature is employed. An approximate value of the integral is obtained analytically for zero, first and second-order ($n = 0, 1, 2$) approximations of the density function $f(y_3) = y_3^\alpha$. Compare the results with those obtained by an alternative method, available for the particular case $\alpha = 1/2$. In this case, the integral is reduced to an elliptic integral which serves us to employ extremely efficient and accurate Carlson algorithms for elliptic integrals [31]. The algorithms provide the benchmark value $J_M^{ext} = -13.84273039$. Table 2 presents obtained numerical results. It also contains data for $\alpha = 5/8$ and $\alpha = 2/3$ with very accurate values obtained by using software *Mathematica*.

Table 2

Values of integral: J_M for approximation of density function by polynomials

approximation	$\alpha = 1/2$	$\alpha = 5/8$	$\alpha = 2/3$
zero order	-13.8349802198	-15.5123882325	-16.1138530746
first order	-13.8350016591	-15.5124182838	-16.1138863768
second order	-13.8438508174	-15.5217211278	-16.1230501171
exact	-13.84273039	-15.52054272	-16.12188862

It can be seen that the second order approximation provides four correct significant digits. This is notably more accurate, than using *fourth-order* approximation on the *entire* trapezoid without distinguishing the thin strip near the field point. Then $J_M = -12.5055392507$, that is the relative error is about 17%.

The method developed has appeared quite efficient and accurate. It is implemented in a subroutine, which may be included into conventional codes of the BEM.

Our experience with square-root edge elements ($\alpha = 1/2$) shows that using special edge and intermediate elements results in significant increasing accuracy of modelling regions of strong field concentration under actually unchanged time expense.

Acknowledgements. The author appreciate the support of the National Science Centre Poland (Project Number 2015/19/B/ST8/00712).

REFERENCES

[1] N.P. Patel and D.S. Sharma, "Composite Structures On the stress concentration around a polygonal cut-out of complex geometry in an infinite orthotropic plate", *Composite Structures*, 179, 415–436, 2017.

[2] A.J. Pachoud, P.A. Manso, and A.J. Schleiss, "New parametric equations to estimate notch stress concentration factors at butt welded joints modeling the weld profile with splines", *Engineering Failure Analysis*, 72, 11–24, 2017.

[3] T. Davis, D. Healy, A. Bubeck, and R. Walker, "Stress concentrations around voids in three dimensions: The roots of failure", *Journal of Structural Geology*, 102, 193–207, 2017.

[4] M. Eskandari-Ghadi, A. Ardeshtir-Behrestaghi, and R.Y.S. Pakc, "Bi-material transversely isotropic half-space containing penny-shaped crack under time-harmonic horizontal loads", *Engineering Fracture Mechanics*, 172, 152–180, 2017.

[5] S. Nategh, A. Khojasteh, and M. Rahimian, "Bonded contact of a rigid disk inclusion with a penny-shaped crack in a transversely isotropic solid", *Journal of Engineering Mathematics*, 110, 123–146, 2018.

[6] V. Maz'ya and B. Plamenevskii, "The coefficients in the asymptotic expansion of solutions of elliptic boundary value problems in domains with conical points", *Math. Nachr.*, 76, 29–60, 1977.

[7] D.B. Bogoy, "Two edge-bonded elastic wedges on different materials and wedge angles under surface tractions", *Journal of Applied Mechanics*, 38 (2), 377–386, 1971.

[8] J.P. Dampsey and G.B. Sinclair, "On stress singularities in the plane elasticity of the composite wedge", *J. Elast.*, 9, 373–391, 1979.

[9] A. Seweryn and Z. Mróz, "A non local stress failure condition for structural elements under multiaxial loading", *Eng. Fracture Mech.*, 51, 955–973, 1995.

[10] G. Mishuris and G. Kuhn, "Comparative study on an interface crack for different wedge interface models", *Arch. Appl. Mechanics*, 71, 764–780, 2001.

[11] G.B. Sinclair, "Stress singularities in classical elasticity", *Appl. Mech. Rev.*, 57, (4–5), 251–297, 385–439, 2004.

[12] V. Blinova and A. Linkov, "A method of finding asymptotic forms at the common apex of elastic wedges", *J. Appl. Math. Mech.*, 59, 187–195, 1995.

[13] A. Linkov and V. Koshelev, "Multi-wedge points and multi-wedge elements in computational mechanics: evaluation of exponent and angular distribution", *Int. J. Solids and Structures*, 71, 764–780, 2005.

[14] A. Linkov and L. Rybarska-Rusinek, "Numerical method and models for anti-plane strain of a system with thin elastic wedge", *Arch. Appl. Mech.*, 78, 821–831, 2008.

[15] A. Linkov and L. Rybarska-Rusinek, "Plane elasticity problem for a multi-wedge system with a thin wedge", *Int. J. Solids and Structures*, 47, 3297–3304, 2010.

[16] A. Linkov and L. Rybarska-Rusinek, "Interface conditions simulating influence of a thin elastic wedge with smooth contacts", *Arch. Appl. Mech.*, 81, 1203–1214, 2011.

[17] A. Linkov and L. Rybarska-Rusinek, "Evaluation of stress concentration in multi-wedge systems with functionally graded wedges", *Int. J. Eng. Sci.*, 61, 87–93, 2012.

[18] E. Rejwer, L. Rybarska-Rusinek, and A. Linkov, "The complex variable fast multipole boundary element method for the analysis of strongly inhomogeneous media", *Eng. Anal. Bound. Elem.*, 43, 105–116, 2014.

[19] H. Li, C. Liu, Y. Mizuta, and M. Kayupov, "Crack edge element of three-dimensional displacement discontinuity method with boundary division into triangular leaf elements", *Comm Numer Meth. Eng.*, 17(6), 365–78, 2001.

[20] L. Rybarska-Rusinek, D. Jaworski, and A. Linkov, "On efficient evaluation of integrals entering boundary equations of 3D potential and elasticity theory", *Journal Math. Appl.*, 37, 85–96, 2014.

- [21] D. Jaworski, A. Linkov, and L. Rybarska-Rusinek, "On solving 3D elasticity problems for inhomogeneous region with cracks, pores and inclusions", *Computers and Geotechnics*, 71, 295–309, 2016.
- [22] D.A. Spence and P.W. Sharp, "Self-similar solutions for elasto-hydrodynamic cavity flow", *Proc. Royal Soc. London, Series A*, 400, 289–313, 1985.
- [23] B. Lenoach, "The crack tip solution for hydraulic fracturing in a permeable solid", *J. Mech. Phys. Solids*, 43, 1025–1043, 1995.
- [24] A. Peirce, "Implicit level set algorithms for modelling hydraulic fracture propagation", *Phil. Trans. R. Soc. A*, 374: 20150423, 2016.
- [25] P.K. Banerjee and R. Butterfield, *Boundary element methods in engineering science*, McGrawHill Book Co., UK, 1981.
- [26] A. Linkov, "Real and complex hypersingular integrals and integral equations in computational mechanics", *Demonstratio Mathematica*, 28 (4), 759–769, 1995.
- [27] D. Nikolskiy, M. Zammarchi, S. Mogilevskaya, and A. Salvadori, "A Three-dimensional BEM analysis of stress state near a crack-borehole system", *Eng. Anal. Bound. Elem.*, 73, 133–143, 2016.
- [28] K. Pierzyński and Ł. Madej, "Numerical modeling of fracture during nanoindentation of the TiN coatings obtained with the PLD process", *Bull. Pol. Ac.: Tech.*, 61 (4), 973–978, 2013.
- [29] J. Rice, "A path-independent integral and the approximate analysis of strain concentration by notches and cracks", *Journal of Applied Mechanics*, 35, 379–386, 1968.
- [30] A. Linkov, "The particle velocity, speed equation and universal asymptotics for the efficient modelling of hydraulic fractures", *J. Appl. Math. Mech.*, 79, 54–63, 2015.
- [31] B. Carlson, "A Table of elliptic integrals: one quadratic factor", *Math Comput*, 56 (193), 267–280, 1999.

Appendix

Formulas for analytical evaluation of integrals for n -order approximation ($n \leq 4$):

$n = 0$

$$I_0 = \int \frac{(ay + b - x_2)dy}{(x_3 - y)^2 \sqrt{(x_3 - y)^2 + (x_2 - ay - b)^2}} = -\frac{\sqrt{(x_3 - y)^2 + (x_2 - ay - b)^2}}{(y - x_3)(ax_3 + b - x_2)} + C$$

$n = 1$

$$I_1 = \int \frac{(ay + b - x_2)dy}{(x_3 - y)\sqrt{(x_3 - y)^2 + (x_2 - ay - b)^2}} = -\log(y - x_3) - \frac{a}{\sqrt{a^2 + 1}} \log\left(\sqrt{(a^2 + 1)\sqrt{(x_3 - y)^2 + (x_2 - ay - b)^2} + a(ay + b - x_3) + y - x_3}\right) + \log\left(\sqrt{(x_3 - y)^2 + (x_2 - ay - b)^2} + ay + b - x_2\right) + C$$

$n = 2$

$$I_2 = \int \frac{(ay + b - x_2)dy}{\sqrt{(x_3 - y)^2 + (x_2 - ay - b)^2}} = \frac{a\sqrt{(x_3 - y)^2 + (x_2 - ay - b)^2}}{a^2 + 1} + \frac{ax_3 + b - x_2}{\sqrt{(a^2 + 1)^3}} + \log\left(\sqrt{(a^2 + 1)\sqrt{(x_3 - y)^2 + (x_2 - ay - b)^2} + a(ay + b - x_3) + y - x_3}\right) + C$$

$n = 3$

$$I_3 = \int \frac{(ay + b - x_2)(x_3 - y)dy}{\sqrt{(x_3 - y)^2 + (x_2 - ay - b)^2}} = \frac{1}{2} \left(\frac{3a(ax_3 + b - x_2)^2}{\sqrt{(a^2 + 1)^5}} \log\left(\sqrt{(a^2 + 1)\sqrt{(x_3 - y)^2 + (x_2 - ay - b)^2} + a(ay + b - x_3)}\right) + \frac{((a - 2a^3)x_3 + a^3y - a^2b + (a^2 - 2)x_2 + ay + 2b)}{(a^2 + 1)^2} \sqrt{(x_3 - y)^2 + (x_2 - ay - b)^2} \right) + C$$

$$n = 4$$

$$\begin{aligned}
 I_4 &= \int \frac{(ay + b - x_2)(x_3 - y)^2 dy}{\sqrt{(x_3 - y)^2 + (x_2 - ay - b)^2}} = \\
 &= \frac{1}{2} \left(\frac{(4a^2 - 1)(ax_3 + b - x_2)^3}{\sqrt{(a^2 + 1)^7}} \log \left(\sqrt{(a^2 + 1) \sqrt{(x_3 - y)^2 + (x_2 - ay - b)^2} + a(ay + b - x_3) + y - x_3} \right) + \right. \\
 &\quad \left. - \frac{(-(a^2 + 1)(2a^2 - 3)(y - x_3)(ax_3 + b - x_2) + a(2a^2 - 13)(ax_3 + b - x_2)^2 + 2a(a^2 + 1)^2(y - x_3)^2)}{3(a^2 + 1)^3} \right. \\
 &\quad \left. \sqrt{(x_3 - y)^2 + (x_2 - ay - b)^2} \right) + C
 \end{aligned}$$